The Environmental Legacy of Copper Metallurgy and Mongol Silver Smelting Recorded in Yunnan Lake Sediments

Aubrey L. Hillman[1], Mark B. Abbott[1], JunQing Yu[2], Daniel J. Bain[1], TzeHuey Chiou-Peng[3]*

[1]Department of Geology and Planetary Science, University of Pittsburgh, 4107 O'Hara St, Pittsburgh, PA 15260, USA

[2]Qinghai Institute of Salt Lake Studies, Chinese Academy of Sciences, 18 Xinning Rd, Xining, Qinghai 810008, China

[3]Spurlock Museum, University of Illinois at Urbana-Champaign, 600 S. Gregory St, MC-065, Urbana, IL 61801, USA

*Corresponding author: alh118@pitt.edu

SUPPORTING INFORMATION

10 pages

5 Figures, 3 Tables

SUPPORTING INFORMATION FIGURES

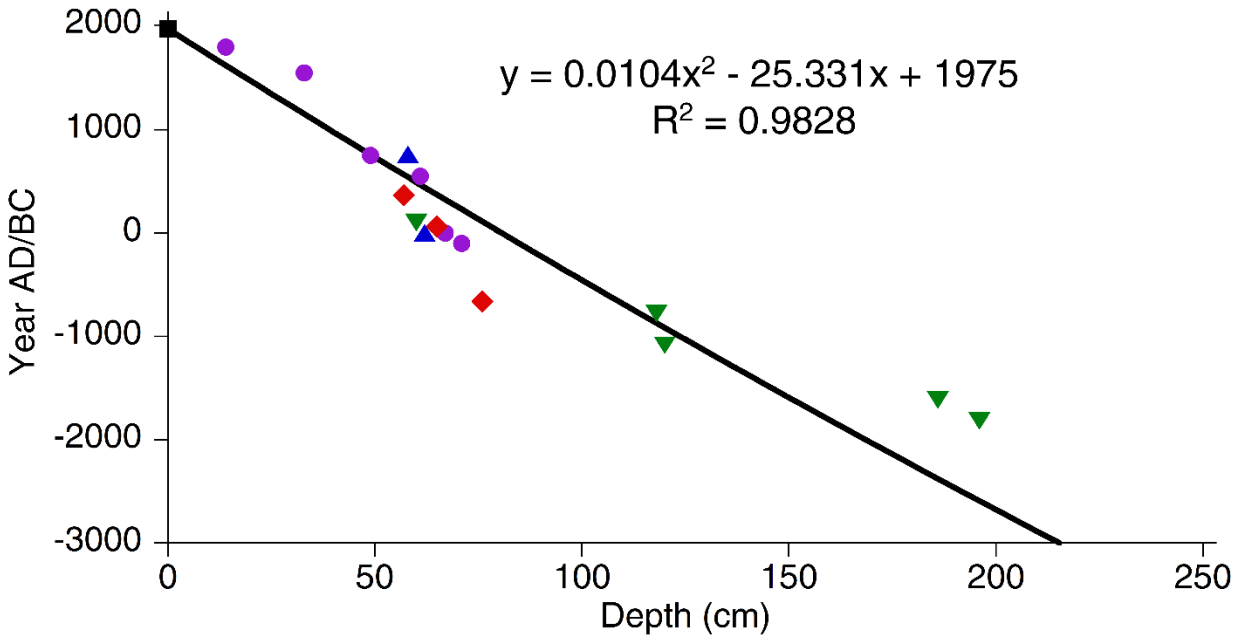

Fig. S1. Dearing et al., (2008) polynomial age model for Erhai sediment cores (collection locations marked in figure 1). Unpublished ^{210}Pb data (black square), paleomagnetic features from Hyodo et al., (1999) (purple circles), terrestrial macrofossil radiocarbon dates (blue triangles), bulk sediment radiocarbon dates from Hyodo et al., (1999) (green inverted triangles), and shell radiocarbon dates from Hyodo et al., (1999) (red diamonds).

Dearing, J. A.; Jones, R. T.; Shen, J.; Yang, X.; Boyle, J. F.; Foster, G. C.; Crook, D. S.; Elvin, M. J. D., Using multiple archives to understand past and present climate–human–environment interactions: the lake Erhai catchment, Yunnan Province, China. Journal of Paleolimnology 2008, 40, (1), 3-31.

Hyodo, M.; Yoshihara, A.; Kashiwaya, K.; Okimura, T.; Masuzawa, T.; Nomura, R.; Tanaka, S.; Xing, T. B.; Qing, L. S.; Jian, L. S., A Late Holocene geomagnetic secular variation record from Erhai Lake, southwest China. Geophysical Journal International 1999, 136, 784-459 790.

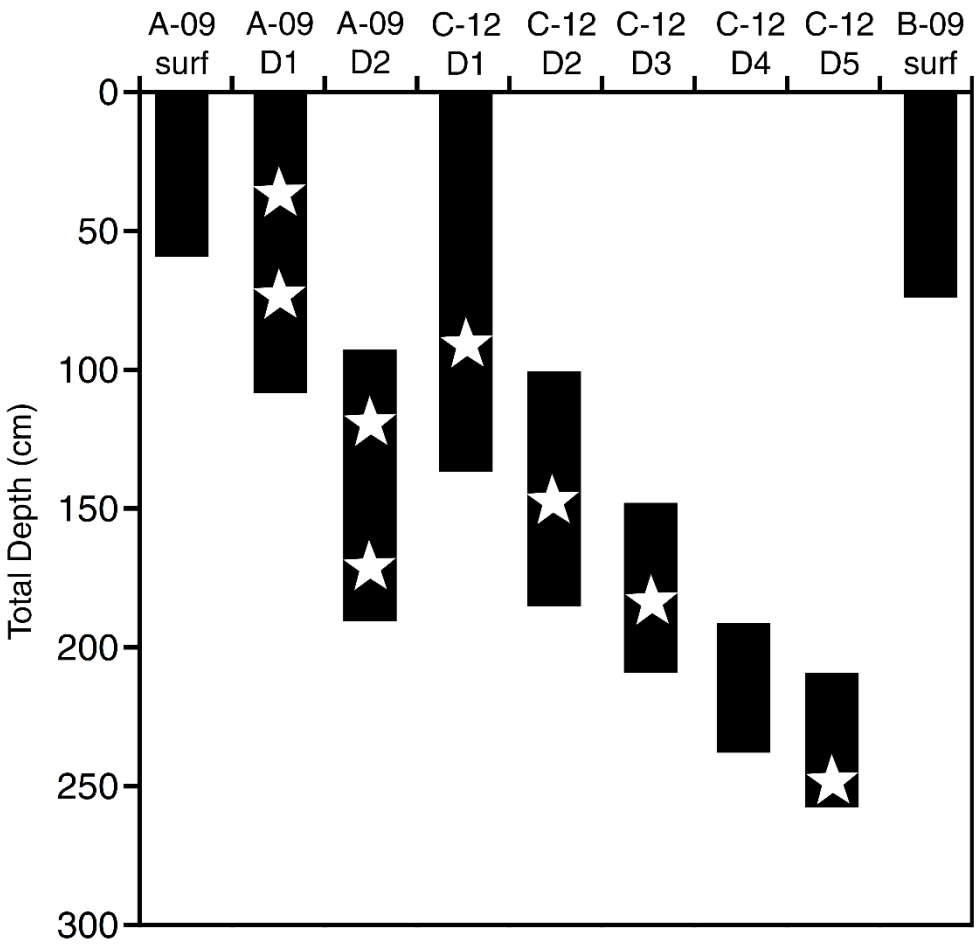

Fig. S2- Total sediment depths of cores from sites A-09, B-09, and C-12 (locations marked in figure 1) and overlapping sections. Terrestrial macrofossil radiocarbon dates marked with white stars (see table S2).

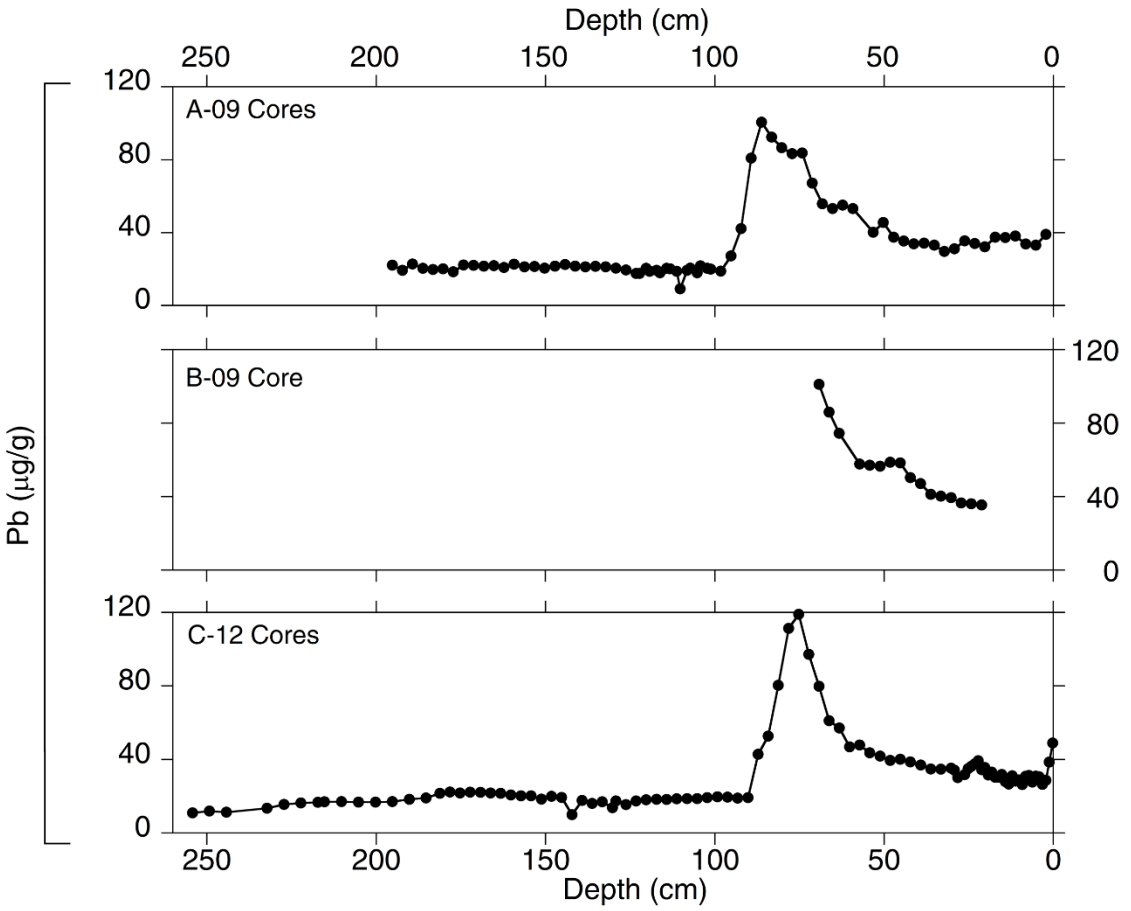

Fig. S3- Lead concentrations by depth for Cores A-09, B-09, and C-12. The increase in Pb occurs at a similar depth and is of a similar magnitude in all three cores, despite their different locations and depths in the lake. Core B-09 is too short to capture the entire increase in Pb.

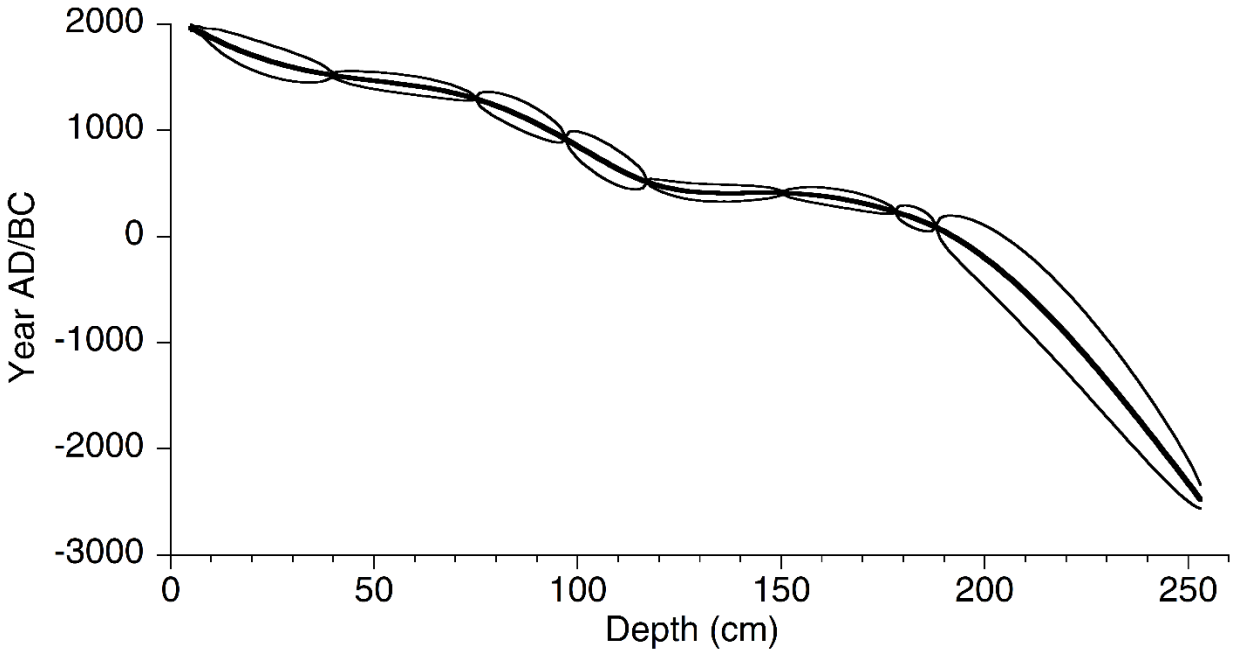

Fig. S4- Results of the age uncertainty analysis with 95% confidence intervals. Age uncertainties were calculated using a 10,000 iteration Monte Carlo similation varied between the radiocarbon 2-sigma calibrated age uncertainties based on methods developed by Marcott et al., (2013) and Huybers et al., (2004). The uncertainty between the age-control points was modeled as a random walk with a "jitter" value of 200.

Marcott, S. A.; Shakun, J. D.; Clark, P. U.; Mix, A. C., A Reconstruction of Regional and Global Temperature for the Past 11,300 Years. Science 2013, 339, (6124), 1198-1201.

Huybers, P.; Wunch, C., A depth-derived Pleistocene age model: Uncertainty estimates, sedimentation variability, and nonlinear climate change. Paleoceanography 2004, 19, PA1028.

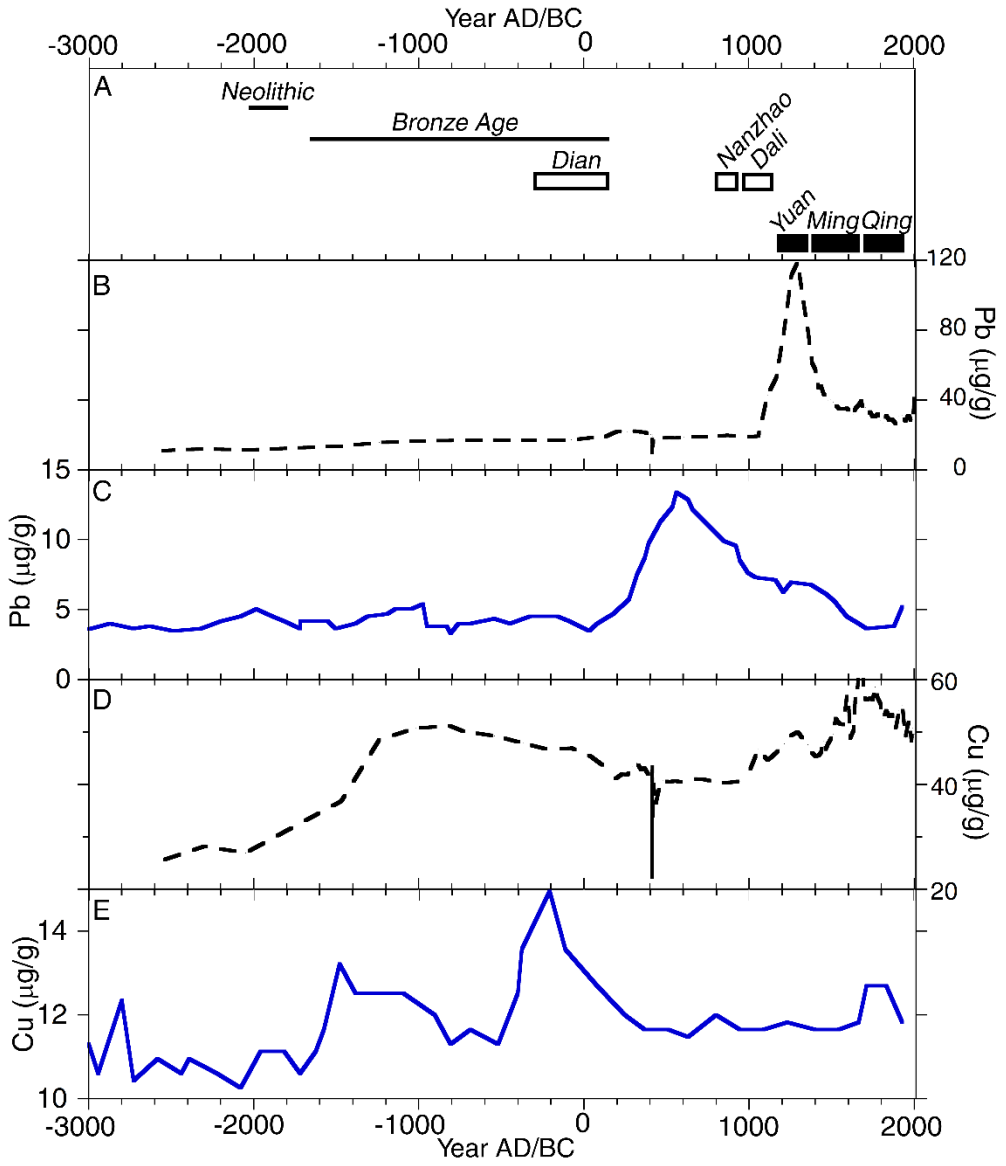

Fig. S5. Comparison between this study and results from Dearing et al., (2008). A- Archaeological periods, Yunnan cultural periods in white boxes, and Chinese dynasties in black boxes, B- concentrations of lead (Pb) from this study (black dashed line), C- concentrations of lead (Pb) from Dearing et al., (2008) (blue solid line), D- concentrations of copper (Cu) from this study (black dashed line), E- concentrations of copper (Cu) from Dearing et al., (2008) (blue solid line). The timing and magnitude of geochemical changes differs significantly between the two studies.

SUPPORTING INFORMATION TABLES

Table S1. AMS radiocarbon dates for samples from Erhai Cores A-09 and C-12.

UCI Number	Composite Core Depth (cm)	Material	^{14}C age (BP)	Error ±	Median Probability Calibrated Age (yr AD/BC)	2σ Calibrated Age Range (yr AD/BC)
Cores A-09						
99742	39.5	Leaf	375	20	1494	1624-1449
99743	75	Wood	700	30	1286	1386-1262
99744	117	Charcoal	1520	70	529	648-406
99873	178	Charcoal	1790	40	235	342-128
Cores C-12						
131495	97.5	Charcoal	1135	20	926	779 - 981
122329	150.5	Leaf	1635	15	414	528 - 355
131496	188.5	Charcoal	1915	20	87	130-33
122330	254.0	Charcoal	4000	20	-2532	-2472 - -2571

Table S2. Down-core ^{210}Pb activities, ^{214}Pb activities, cumulative weight, and CRS sediment ages from Core A-09.

Depth (cm)	^{210}Pb activity, Bq-g^{-1}	1σ Error ^{210}Pb activity	^{214}Pb activity, Bq-g^{-1}	1σ Error ^{214}Pb activity	Cumulative Weight, g cm^{-1}	CRS age (yr AD/BC)	1σ Error Age
Cores A-09							
0.0-0.5	0.3800	0.0610	0.0826	0.0191	0.0425	2003	1.64
1.0-1.5	0.3630	0.0421	0.0514	0.0069	0.1517	1998	1.79
2.0-2.5	0.2990	0.0338	0.0509	0.0053	0.2989	1993	2.02
3.0-3.5	0.1800	0.0203	0.0431	0.0037	0.5921	1985	2.38
4.0-4.5	0.2240	0.0269	0.0509	0.0051	0.8564	1974	3.05
5.0-5.5	0.1350	0.0176	0.0400	0.0040	1.1702	1963	3.94
6.0-6.5	0.1230	0.0145	0.0404	0.0034	1.4822	1950	5.63
7.0-7.5	0.1110	0.0109	0.0460	0.0040	1.8133	1932	9.18
8.0-8.5	0.0866	0.0066	0.0345	0.0033	2.1497	1910	17.83

Table S3. Pearson product-moment correlation coefficient between metals and reference factors over the pre-pollution time period (2700 BC-200 AD) (185-254 cm). The high correlation coefficients between Al, Mg, organic matter and metals of interest demonstrates that Al, Mg, and organic matter are appropriate reference factors from which to calculate EFs as they can explain some component of weathering.

	Al	Mg	Organic Matter
Cu	0.9023	0.9426	0.8904
Pb	0.9579	0.8782	0.9660
Ag	0.8035	0.7448	0.5526
Cd	0.7270	0.6602	0.4702
Zn	0.9646	0.9914	0.9301